

attractor; however, the lattice effect 6-pattern episodically recurs (see Fig. 3, D and E).

The 6-pattern forecast by the stochastic lattice model is evident in the three experimental replicates (3, 18). Figure 4A shows the larval time series data from one replicate. The intermittently occurring 6-pattern is also seen in the phase space representation of the data (Fig. 4B).

Lattice effects can dramatically alter the predictions of ecological models, especially in systems for which the continuous-state deterministic dynamics are complex. In deterministic models, discretizing state space can replace a complicated continuous-state attractor with a simpler lattice attractor; yet the continuous-state dynamics remain important, inasmuch as they continue to shape the transient behavior on the lattice. In the presence of noise, the system is influenced by both transients and attractors, and thus displays episodes that alternately resemble the dynamics of the continuous-state and lattice models. We emphasize that such lattice effects are not only found in relatively coarse lattices or in small populations; indeed, in our experimental study of chaotic population dynamics, lattice effects were important even with  $10^7$  lattice points.

A primary goal of ecology is the understanding of population fluctuations. Our evidence demonstrates that the traditional focus on continuous-state models is too narrow. Specifically, important effects in population dynamics due to the discrete nature of organisms may be entirely missed by continuous-state models, yet follow as straightforward predictions of lattice models. We suggest that a complete understanding of some population systems will require a blend of both continuous-state and discrete-state models.

References and Notes

1. R. M. May, *Science* **186**, 645 (1974).
2. A. Hastings, C. L. Hom, S. Ellner, P. Turchin, H. C. J. Godfray, *Annu. Rev. Ecol. Syst.* **24**, (1993).
3. B. Dennis, R. A. Desharnais, J. M. Cushing, S. M. Henson, R. F. Costantino, *Ecol. Monogr.* **71**, 277 (2001).
4. R. M. May, *Stability and Complexity in Model Ecosystems* (Princeton Univ. Press, Princeton, NJ, ed. 2, 1974).
5. E. A. Jackson, *Perspectives of Nonlinear Dynamics* (Cambridge Univ. Press, Cambridge, 1989), vol. 1, pp. 216–219.
6. H. B. Wilson, M. P. Hassell, *Proc. R. Soc. London B* **264**, 1189 (1997).
7. P. A. P. Moran, *Biometrics* **6**, 250 (1950).
8. W. E. Ricker, *J. Fish. Res. Board Can.* **11**, 559 (1954).
9. R. M. May, G. F. Oster, *Am. Nat.* **110**, 573 (1976).
10. A. J. Nicholson, *J. Anim. Ecol.* **2**, 132 (1933).
11. V. A. Bailey, *Proc. Zool. Soc. London*, 551 (1935).
12. M. P. Hassell, *J. Anim. Ecol.* **69**, 543 (2000).
13. A. C. Crombie, *Proc. R. Soc. London B* **133**, 76 (1946).
14. R. F. Costantino, R. A. Desharnais, *Population Dynamics and the Tribolium Model: Genetics and Demography* (Springer, New York, 1991).
15. C. J. Briggs, S. M. Sait, M. Begon, D. J. Thompson, H. C. J. Godfray, *J. Anim. Ecol.* **69**, 352 (2000).
16. R. N. Chapman, *Ecology* **9**, 111 (1928).

17. J. R. Beddington, C. A. Free, J. H. Lawton, *Nature* **255**, 58 (1975).
18. R. F. Costantino, R. A. Desharnais, J. M. Cushing, B. Dennis, *Science* **275**, 389 (1997).
19. The LPA model is

$$L_{t+1} = bA_t \exp\left(-\frac{c_{ea}}{V}A_t - \frac{c_{el}}{V}L_t\right),$$

$$P_{t+1} = (1 - \mu_l)L_t,$$

$$A_{t+1} = P_t \exp\left(-\frac{c_{pa}}{V}A_t\right) + (1 - \mu_a)A_t.$$

Here  $L_t$ ,  $P_t$ , and  $A_t$  are, respectively, the number of feeding larvae at time  $t$ ; the number of nonfeeding larvae, pupae, and callow adults at time  $t$ ; and the number of sexually mature adults at time  $t$ . The unit of time is 2 weeks, which is the approximate amount of time spent in each of the  $L$  and  $P$  classes under experimental conditions.  $b > 0$  is the average number of larvae recruited per adult per unit time in the absence of cannibalism, and the fractions  $\mu_a$  and  $\mu_l$  are the adult and larval probabilities of dying from causes other than cannibalism in one time unit. The exponentials represent the fractions of individuals surviving cannibalism one unit of time, with "cannibalism coefficients"  $c_{ea}/V$ ,  $c_{el}/V$ ,  $c_{pa}/V > 0$ . Habitat size  $V$  has units equal to the volume occupied by 20 g of flour, the amount of medium routinely used in our laboratory.

20. R. F. Costantino, J. M. Cushing, B. Dennis, R. A. Desharnais, S. M. Henson, *Bull. Math. Biol.* **60**, 247 (1998).
21. R. F. Costantino, J. M. Cushing, B. Dennis, R. A. Desharnais, *Nature* **375**, 227 (1995).
22. J. M. Cushing, B. Dennis, R. A. Desharnais, R. F. Costantino, *Ecol. Model.* **92**, 111 (1996).
23. ———, *J. Anim. Ecol.* **67**, 298 (1998).
24. J. M. Cushing et al., *Chaos Solitons Fractals* **12**, 219 (2001).
25. B. Dennis, R. A. Desharnais, J. M. Cushing, R. F. Costantino, *Ecol. Monogr.* **65**, 261 (1995).
26. ———, *J. Anim. Ecol.* **66**, 704 (1997).
27. R. A. Desharnais, R. F. Costantino, J. M. Cushing, B. Dennis, *Science* **276**, 1881 (1997).
28. R. A. Desharnais, R. F. Costantino, J. M. Cushing, S. M. Henson, B. Dennis, *Ecol. Lett.* **4**, 229 (2001).

29. S. M. Henson, J. M. Cushing, R. F. Costantino, B. Dennis, R. A. Desharnais, *Proc. R. Soc. London B* **265**, 2229 (1998).
30. S. M. Henson, R. F. Costantino, J. M. Cushing, B. Dennis, R. A. Desharnais, *Bull. Math. Biol.* **61**, 1121 (1999).
31. In the experimental protocol, the parameters  $\mu_a$  and  $c_{pa}$  were manipulated by means of the necessarily integerized equation

$$A_{t+1} = \text{int}\left[P_t \exp\left(-\frac{c_{pa}}{V}A_t\right)\right] + \text{int}[(1 - \mu_a)A_t].$$

Thus, one possible deterministic lattice model for the experiment in question, and the one used here, is

$$L_{t+1} = \text{int}\left[bA_t \exp\left(-\frac{c_{ea}}{V}A_t - \frac{c_{el}}{V}L_t\right)\right],$$

$$P_{t+1} = \text{int}[(1 - \mu_l)L_t],$$

$$A_{t+1} = \text{int}\left[P_t \exp\left(-\frac{c_{pa}}{V}A_t\right)\right] + \text{int}[(1 - \mu_a)A_t].$$

32. The stochastic lattice model used here is

$$L_{t+1} = \text{int}\left[\left(\sqrt{bA_t \exp\left(-\frac{c_{ea}}{V}A_t - \frac{c_{el}}{V}L_t\right) + E_{1t}}\right)^2\right],$$

$$P_{t+1} = \text{int}[(\sqrt{(1 - \mu_l)L_t + E_{2t}})^2],$$

$$A_{t+1} = \text{int}\left[P_t \exp\left(-\frac{c_{pa}}{V}A_t\right)\right] + \text{int}[(1 - \mu_a)A_t].$$

where  $E_{1t}$  and  $E_{2t}$  are random normal variables with mean zero and variance-covariance matrix  $\Sigma$ . In the rare cases in which a large negative  $E$  causes a negative value inside a square, we set the right-hand side of that equation equal to zero.

33. We thank E. W. Davis, J. Delos, and W. M. Schaffer for comments. Supported in part by the National Science Foundation (grants DMS 9973126, 9981374, 9981423, 9981458), a Howard Hughes Medical Institute grant to the College of William and Mary (S.M.H.), and an NSF Mathematical Sciences Postdoctoral Research Fellowship (A.A.K.).

12 June 2001; accepted 29 August 2001

## Regulation of Cutaneous Malignancy by $\gamma\delta$ T Cells

Michael Girardi,<sup>1\*</sup> David E. Oppenheim,<sup>2\*</sup> Carrie R. Steele,<sup>2</sup> Julia M. Lewis,<sup>1</sup> Earl Glusac,<sup>1</sup> Renata Filler,<sup>1</sup> Paul Hobby,<sup>3</sup> Brian Sutton,<sup>3</sup> Robert E. Tigelaar,<sup>1</sup> Adrian C. Hayday<sup>2†</sup>

The localization of  $\gamma\delta$  T cells within epithelia suggests that these cells may contribute to the down-regulation of epithelial malignancies. We report that mice lacking  $\gamma\delta$  cells are highly susceptible to multiple regimens of cutaneous carcinogenesis. After exposure to carcinogens, skin cells expressed Rae-1 and H60, major histocompatibility complex-related molecules structurally resembling human MICA. Each of these is a ligand for NKG2d, a receptor expressed by cytolytic T cells and natural killer (NK) cells. In vitro, skin-associated NKG2d<sup>+</sup>  $\gamma\delta$  cells killed skin carcinoma cells by a mechanism that was sensitive to blocking NKG2d engagement. Thus, local T cells may use evolutionarily conserved proteins to negatively regulate malignancy.

A substantial fraction of the T cell pool is constitutively resident within epithelia. These intraepithelial lymphocytes (IELs) display limited T cell receptor (TCR) diversity and may recognize autologous proteins expressed on epithelial cells after infection or malignant transformation (1). Consistent with this, human bowel carcino-

mas show up-regulated expression of two major histocompatibility complex (MHC) class I-related molecules, MICA and MICB, and are targets for cytotoxicity by intestinal TCR $\gamma\delta^+$  IELs expressing NKG2d, a receptor for MICA and MICB (2). Nonetheless, the capacity of either  $\gamma\delta$  cells or MICA to regulate malignancy in vivo is

REPORTS

uncertain. Hence, we have studied three murine models of cutaneous malignancy. The skin was chosen because >90% of murine skin-associated IELs express TCR $\gamma\delta$  (3) and because of the practicality of assessing tumor development in situ. Although the MICA/B locus is not conserved, mice express counterpart NKG2d ligands (4, 5), which might play a role in the detection of tumors.

Malignancy was induced either by inoculation of carcinoma cells or by chemical carcinogenesis. Thus, mice (i) were injected intradermally with the squamous cell carcinoma line PDV into two sites per mouse (6, 7); (ii) were injected intradermally with the carcinogen methylcholanthrene (MCA) (8, 9); or (iii) received skin

applications of dimethylbenz[*a*]anthracene (DMBA) and phorbol ester (12-*O*-tetradecanoylphorbol; TPA), which induce and promote cutaneous malignancy, respectively (10, 11). To directly test the role of  $\gamma\delta$  cells in regulating carcinogenesis, we compared tumor development in wild-type C57BL/6 mice with that in TCR $\delta^{-/-}$  mice, which lack  $\gamma\delta$  cells. Parallel comparisons were made with tumor development in TCR $\beta^{-/-}$  mice, which lack  $\alpha\beta$  T cells, and with TCR $\beta^{-/-}\delta^{-/-}$  mice, which lack all T cells (12).

When wild-type and TCR $\delta^{-/-}$  mice were challenged with PDV cells, the number of sites that had been inoculated and then developed into tumors was greater in the TCR $\delta^{-/-}$  mice by a factor of 3 to 4. In total, 41 of 110 sites developed as tumors in TCR $\delta^{-/-}$  mice, versus 13 of 134 sites in controls ( $P < 0.01$ ). Consistent with this difference, 60% of TCR $\delta^{-/-}$  mice developed at least one tumor, compared to <20% of controls. However, there was only a minor reduction in tumor latency (Fig. 1A), indicating that  $\gamma\delta$  cells reduced the number of events that develop as

tumors, but not the time required for tumor development. In TCR $\beta^{-/-}$  mice and TCR $\beta^{-/-}\delta^{-/-}$  mice, ~100% of sites developed as tumors, and latency was substantially reduced (Fig. 1A). These findings demonstrate that  $\alpha\beta$  T cells and  $\gamma\delta$  cells each regulate the growth of PDV-caused tumors, but in distinct fashions. The susceptible phenotype of TCR $\delta^{-/-}$  mice demonstrates that the lack of  $\gamma\delta$  cells is not compensated for by the presence of  $\alpha\beta$  T cells and NK cells.

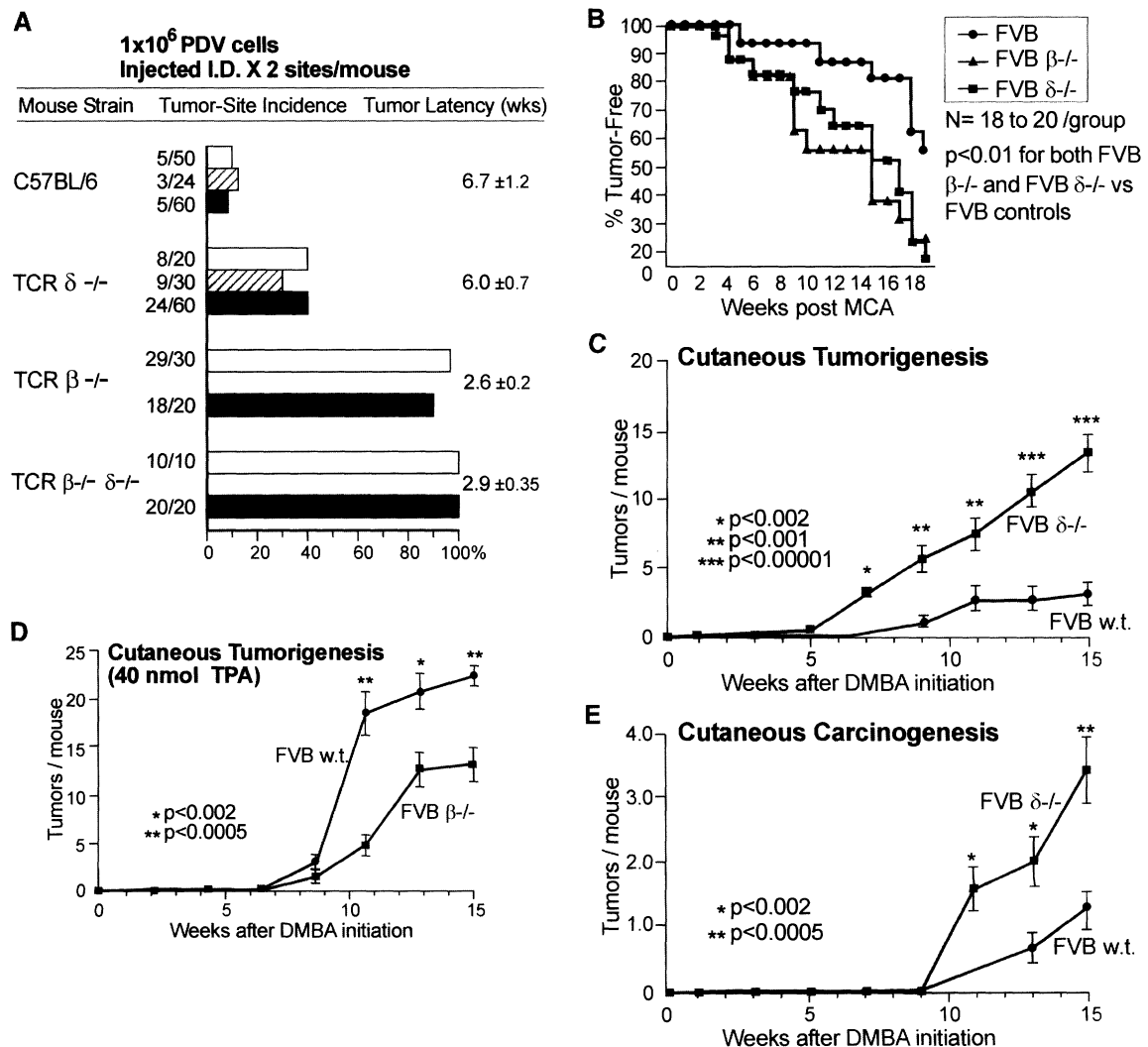
To directly assess the role of  $\gamma\delta$  cells in the development of MCA-induced fibrosarcomas and spindle cell carcinomas, we first backcrossed TCR-mutant mice ( $\geq 11$  generations) to FVB mice, which are highly susceptible to chemical carcinogenesis. After MCA injection, greater numbers of TCR $\delta^{-/-}$  mice and TCR $\beta^{-/-}$  mice developed tumors relative to FVB mice (Fig. 1B). This finding agrees with previous studies showing T cell regulation of MCA-induced skin tumors (13). Again, the presence of either type of T cell failed to compensate for the absence of the other.

Naturally occurring human carcinomas

<sup>1</sup>Department of Dermatology and Yale Skin Diseases Research Core Center, <sup>2</sup>Peter Gorer Department of Immunobiology, Guy's King's St. Thomas' Medical School, <sup>3</sup>Randall Centre for Molecular Medicine, Guy's Hospital, King's College, London SE1 9RT, UK.

\*These authors contributed equally to this report. †To whom correspondence should be addressed. E-mail: adrian.hayday@kcl.ac.uk

**Fig. 1.** Increased cutaneous malignancy in TCR $\delta^{-/-}$  mice. **(A)** Frequency of tumor formation, expressed as numbers of tumors per site of inoculation of  $10^6$  PDV cells and depicted as a percentage. Average latency for the development of palpable tumors is shown in weeks. **(B)** Kaplan-Meier plot of tumor-free FVB mice after single-hit MCA application. **(C)** Number of tumors per mouse developing with time after DMBA initiation and promotion with 5 nmol of TPA (\* $p < 0.002$ , \*\* $p < 0.0001$ , \*\*\* $p < 0.00001$ ). **(D)** As in (C), but with 40 nmol of TPA (\* $p < 0.002$ , \*\* $p < 0.0005$ ). **(E)** Frequency of irregular-shaped carcinomas per mouse after DMBA and 5 nmol of TPA (\* $p < 0.002$ , \*\* $p < 0.0005$ ).



REPORTS

often result from incremental insults that cause an accumulation of mutations (14). This type of etiology can be modeled by application of the tumor initiator DMBA followed by the tumor promoter TPA. Palpable local hyperplasias either regress or develop into regular-shaped papillomas, some of which evolve into irregular-shaped carcinomas (11). At 7 weeks, 67% of TCR $\delta^{-/-}$  mice were tumor-bearing versus 16% of wild-type mice. The tumor burden was also increased in TCR $\delta^{-/-}$  mice (Fig. 1C). By contrast, TCR $\beta^{-/-}$  mice and wild-type mice were equally susceptible to DMBA- and TPA-induced carcinogenesis, and at higher doses of TPA, TCR $\beta^{-/-}$  mice actually showed reduced susceptibility (Fig. 1D). This finding is consistent with other instances where components of the immune response promote rather than inhibit cutaneous malignancy (15). In addition to showing increased tumor burden, TCR $\delta^{-/-}$  mice also revealed a higher incidence of progression of papillomas into carcinomas (Fig. 1E). These experiments provide additional evidence that  $\gamma\delta$  cells and  $\alpha\beta$  T cells make distinct contributions

to the regulation of tumor growth.

In all three regimens,  $\gamma\delta$  cell deficiency reduced resistance to cutaneous malignancy. To determine whether the tumor cells might express a functional equivalent of human MICA/B that could act as a ligand for NKG2d on  $\gamma\delta$  cells, we constructed streptavidin beads displaying the ectodomains of recombinant murine NKG2d fused to a stalk provided by domains 3 and 4 (d3+4) of rat CD4 (16–18). These beads bound PDV cells (Fig. 2A). Mouse cells staining with NKG2d reagents have previously been shown to express the MHC class I-related proteins Rae-1 or H60 (4, 5, 19). Sequence analysis of RNA expressed by PDV cells identified Rae-1 $\epsilon$  (Fig. 2B) (20–22), a novel fifth sequence encoded by the Rae-1 locus (Fig. 2C) (21). Rae-1 proteins are glycosylphosphatidylinositol (GPI)-linked (4, 5, 21); consistent with this fact, PDV cell staining by NKG2d beads was sensitive to the presence of phospholipase C (Fig. 2A).

To test whether murine NKG2d could directly interact with Rae-1 $\epsilon$ , we immobilized Rae-1 $\epsilon$ -CD4(d3+4) fusion protein on beads

(23) that were incubated with recombinant NKG2d-CD4(d3+4). We observed that 110-kD homodimers of NKG2d-CD4(d3+4) were retained efficiently on the Rae-1-CD4 beads but inefficiently on control beads displaying CD4(d3+4) (Fig. 3B). A specific interaction between soluble Rae-1 $\epsilon$  and immobilized NKG2d was confirmed by surface plasmon resonance (Fig. 3C) (24).

The hypothesis that the Rae-1-NKG2d interaction is homologous to that of human NKG2d and MICA was tested by molecular modeling. Fold recognition identified the best template for Rae-1 to be the MHC-like molecule ZAG (25, 26). When this model is compared with the crystal structure of MICA complexed to NKG2d (27), it is clear that the charge distribution and contours of surfaces of MICA and Rae-1 are similar and are quite distinct from those of conventional class I MHC (22). Likewise, the residues in human NKG2d that contact MICA are conserved and appropriately located in murine NKG2d (27, 28). Molecular phylogenetic analysis confirmed the relatedness of Rae-1 to MICA/B and to the recently described human ULBP proteins that also bind NKG2d (Fig. 3D) (29).

To determine whether cutaneous TCR $\gamma\delta^{+}$  IELs [known as dendritic epidermal T cells (DETCs)] can respond to Rae-1 expression on PDV cells, we tested DETCs for NKG2d expression. By reverse transcription polymerase chain reaction (RT-PCR), NKG2d was detected at very low levels in a primary interface epidermal cell (IEC) preparation that contains 1% DETC (“crude IEC”), but was more clearly apparent in enriched IEC composed of ~4% DETC (Fig. 3A). NKG2d was expressed in all DETC lines and was slightly enhanced by cell activation (5, 30). Two recently and independently derived DETC lines, 10-21 and 6-13, were tested for cytolytic effector function toward PDV cells (31, 32). Killing was consistently evident, even at an effector:target (E:T) ratio of 0.3:1 (Fig. 4A). As the E:T ratio was substantially increased, greater cytotoxicity ( $\leq 80\%$ ) was occasionally observed (33), although there was greater experimental variation, perhaps due to T cell inhibition by-products released from dying tumor cells.

To investigate the molecules mediating the targeting of PDV cells by DETCs, we supplemented killing assays with soluble antibody to TCR $\gamma\delta$ , soluble recombinant Rae-1 $\epsilon$ , or an antiserum to NKG2d (34). Each reagent significantly inhibited killing (Fig. 4A). Moreover, the combination of anti-TCR $\gamma\delta$  with either of the other two reagents reduced killing additively by 75 to 95% (Fig. 4A). These results are consistent with recent experiments showing that killing of virus-infected cells by NKG2d $^{+}$   $\alpha\beta$

**Fig. 2.** A cell surface ligand for murine NKG2d. (A) Left panel: PDV cells stained with NKG2d beads (dark shading) and unstained (light shading). Right panel: staining of PDV cells by NKG2d beads after 60-min pretreatment of cells with phospholipase C (dark shading) and unstained (light shading). (B) Rae-1 RT-PCR products detected by ethidium bromide staining in agarose. (C) Predicted amino acid alignment (40) of Rae-1 isoforms. The boxed residues are four charged residues that are conserved in corresponding positions in MICA where they contact homodimeric NKG2d (note that one of the four is not completely conserved in Rae-1); asterisks are primary sites of divergence between isoforms; putative N-linked glycosylation sites are underlined and in bold; italics in Rae-1 $\epsilon$  denote primer sequences used to clone the cDNA; cysteines are in yellow; STP denotes a serine-threonine-proline-rich domain;  $\alpha$  helix and  $\beta$  sheets, kinks, and loops are designated on the basis of the structural model (22).

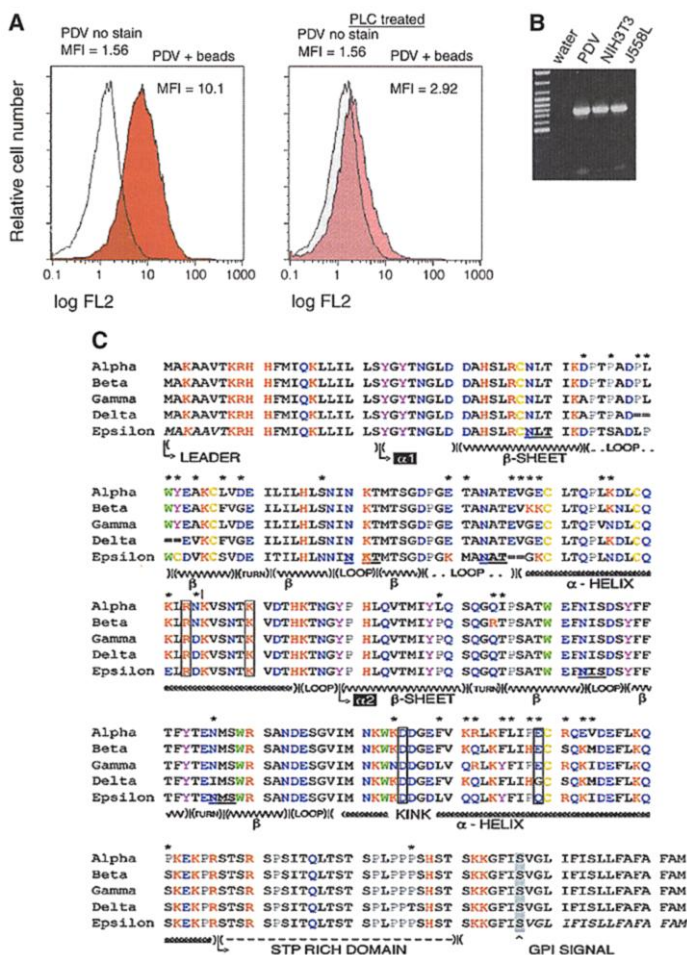


**Fig. 3.** NKG2d is expressed on TCR $\gamma\delta^+$  cells and binds Rae-1 $\epsilon$ . (A) NKG2d expression in TCR $\gamma\delta^+$  DETC lines [7-17, B1, 30B4, and U10E1, maintained as resting cultures or stimulated with anti-CD3 ( $\alpha$ CD3)]; in transformed keratinocyte cell lines (PAM2-12, PDV); and in epidermal preparations directly ex vivo (crude IEC) and in those enriched for primary DETC cells (enriched IEC). (B) Biochemical evidence for Rae-1 $\epsilon$  binding to NKG2d was provided by use of magnetic streptavidin beads coated with either biotinylated recombinant CD4(d3+4) (CD4 bead) or a fusion of CD4(d3+4) with Rae-1 $\epsilon$  (Rae-1 $\epsilon$  bead). After a 5-hour incubation of beads with 100 nmol of NKG2d-CD4(d3+4), proteins were eluted from the beads with SDS or were sampled from the unbound supernatant and detected by Western blotting using OX68 (anti-CD4). The ~110-kD NKG2d-CD4(d3+4) homodimer is detected most strongly in the supernatant of the CD4 beads and the bound fraction of the Rae-1 $\epsilon$  beads. Eluted Rae-1 $\epsilon$ -CD4(d3+4) is detected at ~76 kD. (C) Surface plasmon resonance indicates specific binding of Rae-1 $\epsilon$ -CD4 to NKG2d-CD4. Dark lines are increasing concentrations of Rae-1 $\epsilon$  analyte: 4, 8, 16, and 32  $\mu$ M; faint dotted line is CD4 analyte, 8  $\mu$ M. (D) Phylogeny of MHC class I-related molecules generated with the topological algorithm of ClustalW (Rae-1 $\epsilon$  and H60 are highlighted).

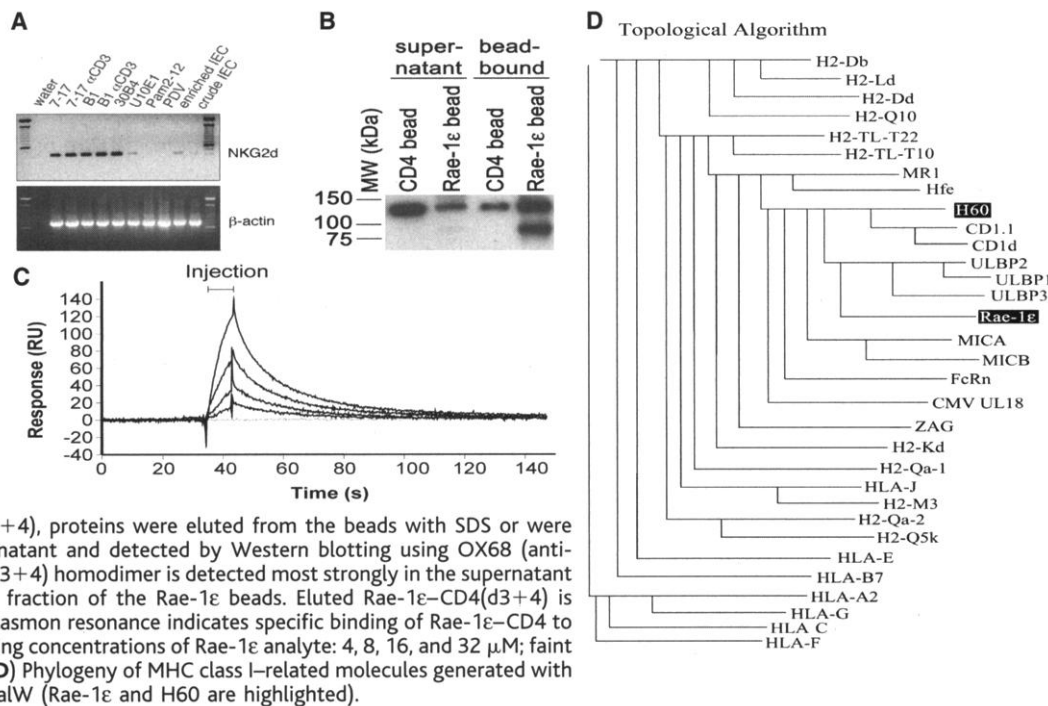
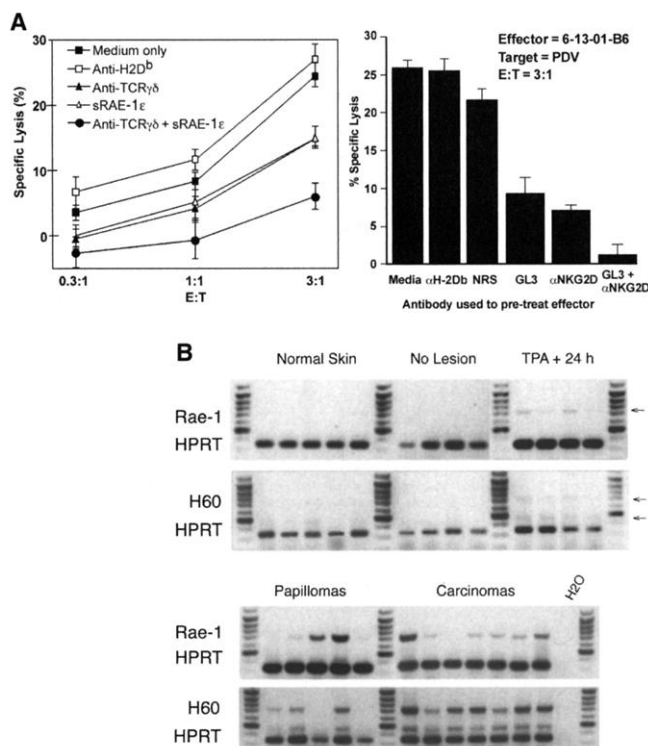


**Fig. 4.** Targeting of Rae-1 $^+$  cells by  $\gamma\delta$  cells and Rae-1 expression in vivo. (A) Left panel: Chromium release assay of  $^{51}$ Cr-loaded PDV cells after incubation with TCR $\gamma\delta^+$  DETC, in the presence of the indicated reagents (sRAE-1 $\epsilon$  = soluble recombinant Rae-1 $\epsilon$  produced in 293T cells). Right panel: Killing at E:T 3:1, with anti-H2D $^b$ , anti-TCR $\gamma\delta$  (GL3), anti-NKG2d, or normal rat serum. (B) RT-PCR products for HPRT, Rae-1, and H60 in individual samples of normal skin, skin treated with TPA and harvested several weeks later in the absence of overt lesion, skin treated with TPA and sampled 24 hours later, papillomas, and carcinomas. HPRT controls were performed in the same reaction and are present in each lane, irrespective of the expression of H60 or Rae-1; H60 gives rise to two transcripts detected as two fragments, as described (19). Detection was by ethidium bromide staining, shown in reverse image.



moderately increased in several areas of painted skin 24 hours after surface application of TPA. Where such areas did not develop any histological lesions, there was subsequently no evidence for Rae-1 or H60 expression. By contrast, Rae-1 and/or H60 were expressed in most freshly explanted papillomas and in all carcinomas.

The high susceptibility of immunosuppressed renal graft patients to squamous cell carcinomas is well established (37). By contrast, the individual immunological mechanisms that contribute to tumor surveillance are not fully defined. In this study, mice lacking  $\gamma\delta$  cells are shown to have increased susceptibility to three distinct regimens of induced cutaneous malignancy. Moreover, there are clear differences in the nature of the contributions that  $\gamma\delta$  cells and  $\alpha\beta$  T cells make to the regulation of malignancy induced by PDV cells and by application of DMBA and TPA.

In species as diverse as chickens, mice, and humans, local T cell subsets are commonly enriched in  $\gamma\delta$  cells. Here we have shown that TCR $\gamma\delta^+$  DETCs can kill squamous carcinoma cells, contingent on the expression of Rae-1 by these cells. Consistent with the capacity of  $\gamma\delta$  cells to inhibit tumor development, we have shown that Rae-1 is up-regulated in vivo by chemical carcinogens. Because NKG2d is expressed on numerous cytolytic T cells and NK cells, transformed cells expressing NKG2d ligands such as Rae-1 and MICA may be vulnerable to several types of attack. It is likely that the nature of the cells that target tumor cells in vivo is determined by the anatomical accessibility of the tumor to the

T cells is contingent on the engagement of NKG2d and TCR (35).

To assess the general relevance of NKG2d-dependent killing of PDV to the immune surveillance of carcinomas, we examined the expression of Rae-1 by RT-PCR in normal FVB skin, in skin treated with DMBA

and TPA, in papillomas, and in carcinomas (11, 36). Normal skin showed negligible levels of Rae-1, consistent with evidence that Rae-1 is primarily expressed in embryonic brain and limb buds (21). There was likewise no evidence of H60 expression (Fig. 4B). By contrast, Rae-1 and H60 expression were

NKG2d<sup>+</sup> cell and the presence of other ligands on the transformed cells that might either activate or inhibit particular types of cytolytic cell. In the case of cutaneous malignancy in the mouse, the nonredundant contribution of  $\gamma\delta$  cells may reflect the intimate juxtaposition of DETC with keratinocytes and/or the presence on keratinocytes of an as-yet-unidentified ligand for the  $\gamma\delta$  TCR.  $\gamma\delta$  T cells may perform similar roles in the human gut, where NKG2d<sup>+</sup> TCR $\gamma\delta$ <sup>+</sup> IELs are highly cytolytic (2), and in human skin, where a distinct subset of  $\gamma\delta$  T cells was recently identified (38).

DETC-mediated cytotoxicity may complement the interferon  $\gamma$ -mediated effects that were recently shown to contribute to immunosurveillance of MCA-induced tumors (13). Additionally, TCR $\gamma\delta$ <sup>+</sup> DETC can down-regulate inflammation provoked by systemic  $\alpha\beta$  T cells (39). Because  $\alpha\beta$  T cell responses can on occasion promote tumor growth (15), as shown for the DMBA-TPA regimen studied here, their down-regulation may be another means by which local  $\gamma\delta$  cells may reduce primary tumor development. These findings are clearly relevant to understanding the selective pressures on developing tumors and to considering the types of immune responses that would be useful in clinical intervention.

References and Notes

1. C. A. Janeway, B. Jones, A. Hayday, *Immunol. Today* **9**, 73 (1988).
2. V. Groh et al., *Proc. Natl. Acad. Sci. U.S.A.* **96**, 6879 (1999).
3. D. Asarnow et al., *Cell* **55**, 837 (1988).
4. A. Cerwenka et al., *Immunity* **12**, 721 (2000).
5. A. Diefenbach, A. Jamieson, S. Liu, N. Shastri, D. Raulet, *Nature Immunol.* **2**, 119 (2000).
6. N. Fusenig, S. Amer, P. Boukamp, P. Worst, *Bull. Cancer* **65**, 271 (1978).
7. PDV cells were trypsinized, washed three times, and resuspended in phosphate-buffered saline before intradermal injection (i.e., raising a bleb) with a 25-gauge needle into C57BL/6 mice at 10<sup>6</sup> cells per site. Mice were observed weekly for palpable tumors, which were measured with calipers in two directions to determine tumor area. Mice were killed for tumors measuring greater than 100 mm<sup>2</sup>. All experiments using animals were carried out in facilities accredited by the Association for Assessment and Accreditation of Laboratory Animal Care.
8. D. Kaplan et al., *Proc. Natl. Acad. Sci. U.S.A.* **95**, 7556 (1998).
9. Wild-type, TCR $\delta$ <sup>-/-</sup>, and TCR $\beta$ <sup>-/-</sup> C57BL/6 mice (Jackson) were backcrossed to FVB (Taconic) for  $\geq$ 11 generations. Repeat testing failed to identify known bacterial pathogens, mites, or pinworms on the skin. All mice used were ~8 weeks of age. Mice were injected intradermally (i.e., raising a visible bleb) with 5  $\mu$ g of 3-MCA (Fluka) in 100  $\mu$ l of peanut oil (Sigma) into the right flank using a 3/4-inch 27-gauge needle. Mice were inspected and tumors examined every 1 to 2 weeks (7).
10. D. Owens, S. Wei, R. Smart, *Carcinogenesis* **20**, 1837 (1999).
11. Initiation was by pipette application of 100 nmol of DMBA (Sigma) in acetone onto the back skin of 8-week-old mice, 1 week after shaving hair with electric clippers. Promotion was weekly with 5 or 40 nmol of TPA (Sigma). Mice were assessed every 1 to 2 weeks for tumor development, and tumors

were counted and scored as clinically apparent papillomas (typically well-demarcated, symmetrical, pedunculated, or dome-shaped papules, without erosion or ulceration) or clinically apparent carcinomas (poorly demarcated, asymmetrical, nonpedunculated, or dome-shaped papules with erosion or ulceration).

12. P. Mombaerts et al., *Nature* **365**, 53 (1993).
13. V. Shankaran et al., *Nature* **410**, 1107 (2001).
14. D. Hanahan, R. Weinberg, *Cell* **100**, 57 (2000).
15. L. Coussens, Z. Werb, *J. Exp. Med.* **193**, F23 (2001).
16. To express biotinylated type II integral membrane proteins COOH-terminal to d3+4 of rat CD4, we modified plasmid pBSKS-XB (17). The resulting vector, pBSKS type II (containing Xba I-CD4L-Sal I-BirA-Xma I-CD4 d3+4-Eco RI-stop-Bam HI), was designed such that the synthetic BirA substrate peptide SGSLHHILDAQKMWVNHNR (40) is NH<sub>2</sub>-terminal to the mature protein. Murine NKG2d cDNA, amplified from C57BL6 lymph node using primers GGAA-7TCAGCGCGCGGCTCTCTTTCAGCCAGTATTGTGCAAC and GATATCTGATCAAGATCTTTACACCGCCCTT-TTCATGCAG, was ligated into the pBSKS Type II vector via Eco RI and Bam HI. The coding fragment (Xba I-Bgl II) was subcloned into the expression vector pEF-BOS (18). Recombinant proteins were expressed in 293T cells with supernatants harvested at 72 hours and again 72 hours later. Harvests were assayed by Western blot with OX68 (antibody to rat CD4) and by CD4-inhibition ELISA (enzyme-linked immunosorbent assay); NKG2d chimeras were routinely expressed at ~20  $\mu$ g/ml. On nonreduced SDS gels, NKG2d-CD4d3+4 chimeras ran at ~110 kD. For biotinylation, supernatants were exchanged 1:100 into 10 mM tris-HCl (pH 8.0) and concentrated for addition of 1  $\mu$ l of BirA biotin ligase (Avidity) per 0.7 ml of concentrate. Unreacted biotin was removed by dialysis. Biotinylation was assessed by depletion with avidin-coated beads and OX68 Western blot of residual supernatants. For cell staining, 200  $\mu$ l of avidin-coated 0.5- $\mu$ m pink fluorescent particles (Spherotech) were resuspended in 400  $\mu$ l of biotin-CD4-NKG2d for 1 to 2 hours at 4°C, pelleted, and resuspended in 200  $\mu$ l of RPMI medium. PDV cells were dissociated by agitation and 0.5 mM EDTA. Treatment with PLCgamma (5 U/ml, Sigma) was for 1 hour at 37°C with mixing every 10 min. Cell staining took place on ice for 1 hour with mixing. Tubes were flooded with 1.5 ml of RPMI; cells were pelleted by centrifugation and analyzed in a Coulter or Cytomation MoFlo flow cytometer.
17. M. H. Brown et al., *J. Exp. Med.* **188**, 2083 (1998).
18. S. Mizushima, S. Nagata, *Nucleic Acids Res.* **18**, 5322 (1990).
19. S. Malarkannan et al., *J. Immunol.* **161**, 3501 (1998).
20. Rae-1 $\epsilon$  cDNA was amplified from PDV cells using primers AAAATCTAGAGAAACCATGGCCAAAGGCAGC-AGTGACC and AAAATGTCCAGCCAGATATGAAGATGAGTCCCACAGAG. The GenBank accession number for Rae-1 $\epsilon$  is AY056835.
21. M. Nomura et al., *J. Biochem. (Tokyo)* **120**, 987 (1996).
22. Supplementary information is available at Science Online ([www.sciencemag.org/cgi/content/full/1063916/DC1](http://www.sciencemag.org/cgi/content/full/1063916/DC1)).
23. Rae-1 $\epsilon$  cDNA was cloned into the Xba I-Sal I sites of the Type I pEF-BOS vector containing CD4 d3+4 and the BirA substrate peptide. Magnetic beads were coated with either biotinylated Rae-1 $\epsilon$  CD4 d3+4 or CD4 d3+4 and incubated with 2 nmol of nonbiotinylated NKG2d for 5 hours at 4°C with rocking before pelleting on a magnet. Bound and unbound proteins were determined after dissociation by SDS-polyacrylamide gel electrophoresis (PAGE) and Western blotting with OX68. Nonbiotinylated NKG2d and Rae-1 $\epsilon$  were affinity-purified on an OX68 column and acid-eluted in 0.2 M acetate, 500 mM NaCl buffer. After neutralization, proteins were concentrated, run on SDS-PAGE, and silver-stained to assess purity. Protein concentrations were measured by BCA protein assay (Sigma).
24. Surface plasmon resonance experiments were done in the biacore-X (Biacore AB). Dilutions of Rae-1 $\epsilon$  analyte in HBS-P (Biacore AB) with 5 mM calcium

were injected over 7 s at 100  $\mu$ l/min into flow cells containing 500 RU of biotinylated NKG2d coupled to a streptavidin-coated chip or a reference cell containing ~500 RU of biotinylated CD4 domains 3 and 4. Rae-1 $\epsilon$  analytes were gel-filtered just before experiments.

25. L. M. Sanchez, A. J. Chirino, P. Bjorkman, *Science* **283**, 1914 (1999).
26. Candidate template structures for Rae-1 were identified using the fold recognition program 3dPSSM. ZAG (PDB code 1ZAG) gave the highest score; other MHC-related molecules also scored highly. The Rae-1 sequence was threaded onto template C $\alpha$  traces, and full coordinates were generated using the program HOMOLOGY (in INSIGHT, Molecular Simulations Inc.), with loops modeled with GENLOOP where necessary. A phylogenetic tree was generated using the multi-sequence alignment ClustalW and GeneBee bioinformatics resources (<http://genebee.msu.su>).
27. P. Li et al., *Nature Immunol.* **2**, 443 (2001).
28. D. W. Wolan et al., *Nature Immunol.* **2**, 248 (2001).
29. D. Cosman et al., *Immunity* **14**, 123 (2001).
30. E. L. Ho et al., *Proc. Natl. Acad. Sci. U.S.A.* **95**, 6320 (1998).
31. J. Coligan et al., *Current Protocols in Immunology* (Wiley, New York, 1991).
32. Soluble Rae-1 $\epsilon$  was prepared as described (24) and used at a final concentration of 1  $\mu$ g/ml.
33. J. M. Lewis, R. E. Tigelaar, unpublished data.
34. Rats were immunized with recombinant murine NKG2d-rat CD4d3+4 chimera purified to homogeneity, as detected by silver staining of electrophoresed protein (24). The antiserum recognized the immunogen in ELISA and Western blots, with negligible reactivity toward CD4 d3+4. It immunoprecipitated one specific species from DETC lines, by comparison with normal rat serum.
35. V. Groh et al., *Nature Immunol.* **2**, 255 (2001).
36. RNA was prepared by trizol (Gibco) from cell pellets, from adherent cells lysed in flasks, from fresh organ samples homogenized directly into trizol using an electric homogenizer, from normal skin, or from skin lesion samples that were snap-frozen in liquid nitrogen and ground with mortar and pestle. Conditions for all standard PCRs: 3 min at 96°C (45 s at 96°C, 45 s at 56°C, 1 min at 72°C), 30 cycles; 10 min at 72°C. PCR primers for mouse H60: sense, GAAGAC-CATGGCAAAGGGAGCC; antisense, TTTTCTTCAG-CATACCCAAGCGAATACC (products are 774 and 550 bp); Rae-1: sense, GAAACCATGGCCAAAGGCAG-CAGTGACC; antisense, AGATATGAAGATGAGTCCC-ACAGAG (product is 762 bp); hypoxanthine-guanine phosphoribosyltransferase (HPRT): forward, GTTG-GATACAGCCAGACTTTGTTG; reverse, GAGGG-TAGGCTGGCTATGGCT (product is 352 bp);  $\beta$ -actin: sense, CTGAAGTACCCCATGGAACATGGC; antisense, CAGAGCAGTAATCTCCTTCTGCAT (product is 762 bp).
37. V. Marshall, *Transplantation* **17**, 272 (1974).
38. W. Holtmeier et al., *J. Invest. Dermatol.* **116**, 275 (2001).
39. M. Girardi, J. Lewis, A. C. Hayday, R. E. Tigelaar, unpublished data.
40. Single-letter abbreviations for amino acid residues are as follows: A, Ala; C, Cys; D, Asp; E, Glu; F, Phe; G, Gly; H, His; I, Ile; K, Lys; L, Leu; M, Met; N, Asn; P, Pro; Q, Gln; R, Arg; S, Ser; T, Thr; V, Val; W, Trp; and Y, Tyr.
41. We thank A. Balmain for PDV cells and for discussions on oncology regimens; M. Brown for help with the development of polyvalent staining reagents; J. Steel for generating antisera; many colleagues, particularly A. Turner for advice; and W. Turnbull for flow cytometry. Supported by Wellcome Trust grant 05308 (A.C.H.), NIH AI grant 27855 (R.E.T.), and an NIH KO8 grant (M.G.). C.R.S. is a HHMI predoctoral fellow.

29 June 2001; accepted 4 September 2001  
 Published online 20 September 2001;  
 10.1126/science.1063916  
 Include this information when citing this paper.